Feasibility of MR-Temperature Mapping of Ultrasonic Heating from a CMUT

Serena H. Wong, Ronald D. Watkins, *Member, IEEE*, Mario Kupnik, *Member, IEEE*, Kim Butts Pauly, and Butrus T. Khuri-Yakub, *Fellow, IEEE*

***Abstract*—In the last decade, high intensity focused ultrasound (HIFU) has gained popularity as a minimally invasive and noninvasive therapeutic tool for treatment of cancers, arrhythmias, and other medical conditions. HIFU therapy is often guided by magnetic resonance imaging (MRI), which provides anatomical images for therapeutic device placement, temperature maps for treatment guidance, and postoperative evaluation of the region of interest. While piezoelectric transducers are dominantly used for MR-guided HIFU, capacitive micromachined ultrasonic transducers (CMUTs) show competitive advantages, such as ease of fabrication, integration with electronics, improved efficiency, and reduction of self-heating. In this paper, we will show our first results of an unfocused CMUT transducer monitored by MR-temperature maps. This 2.51 mm by 2.32 mm, unfocused CMUT heated a HIFU phantom by 14°C in 2.5 min. This temperature rise was successfully monitored by MR thermometry in a 3.0 T General Electric scanner.**

I. Introduction

High intensity focused ultrasound (HIFU) has gained popularity in medical procedures because it can be focused onto a region of interest without harming intervening tissues. Focusing allows ultrasound to be applied noninvasively or minimally invasively, with low morbidity and mortality [1]. HIFU is being investigated for neurological treatments of the central nervous system [2], [3], arrythmia treatments in the heart [4]–[7], drug delivery [8], and coagulation for deep internal bleeding [9], [10]. HIFU cancer treatments of the bone, brain, breast, liver, kidneys, prostate, and uterine fibroids are receiving increased interest; progress in these treatments is reviewed in [11].

Magnetic resonance imaging (MRI) is one of the dominant imaging modalities for guidance of HIFU cancer treatments; MR-guided HIFU systems are used extensively to treat uterine fibroids [12]–[16]. These table-top systems also have demonstrated the feasibility of HIFU in pig livers [13], [17]. MR images provide three essential functions: 1) anatomical image guidance for placement of the HIFU probe, 2) real-time temperature monitoring using proton resonance frequency shift to target the location and duration of the therapy [18]–[20], and 3) post-process functional assessment to evaluate the degree of tissue necrosis [21]. The second function, temperature monitoring, is critical because local perfusion is variable and cannot be predicted [22].

Other imaging modalities do not accurately monitor the thermal dose or identify the necrosed tissue. While ultrasound imaging shows an increasing hyperechogenic area during treatment, this region does not correspond to ablated tissue and often obscures the tumor [23]. Also, ultrasound cannot delineate remaining viable tumor [24]. Contrast enhanced computer tomography (CT) can identify the region of tumor necrosis. However, this area cannot be imaged repeatedly or in real time during the treatment.

Although quartz crystals with converging lenses were used for HIFU in the 1950s [25], compound piezoelectric transducers have been dominant for the past 50 years. Compared to quartz crystals, piezoelectric materials are easily formed into spherical shapes, which allow mechanical focusing and eliminate coupling through a lens [26]. Since the 1950s, many research groups have been optimizing and customizing compound piezoelectric-based materials for high power applications [27], [28]. With these materials, both single-element unfocused [29], [30] and mechanically focused [26], [31], piezoelectric transducers have been used for therapeutics in the heart, liver, and kidney, to name a few. Transducer arrays have also been developed for dynamic electronic focusing of therapy [5], [32]–[34].

Though piezoelectric transducers have been traditionally used for HIFU, capacitive micromachined ultrasonic transducers (CMUTs) have become highly competitive with regard to fabrication and performance. Because CMUTs are fabricated using a silicon micromachining process with sub-micron accuracy, they can be easily fabricated for a broad range of frequencies and sizes [35]. In addition, CMUTs are easily integrated with electronics, either monolithically or through flip-chip bonding [35]. In terms of performance, CMUTs have wide bandwidth in immersion and a high efficiency [36], [37]. In addition to these well-known benefits, CMUTs do not suffer from self-heating effects because they are fabricated from highly thermally conductive silicon. This makes CMUTs well suited for high power and continuous wave (CW) applications such as HIFU [38], [39].

Our goal is to develop noninvasive and minimally invasive HIFU CMUTs for applying therapy under MR-guidance. The configuration of these focused transducers will be determined by the anatomy of the region of inter-

Manuscript received August 23, 2007; accepted November 19, 2007. This research is supported by NIH R01 CA77677 and R01 CA 121163.

S. H. Wong, M. Kupnik, and B. T. Khuri-Yakub are with the Edward L. Ginzton Laboratory, Stanford University, Stanford, CA (e-mail: shwong@stanford.edu).

R. D. Watkins and K. Butts Pauly are with the Department of Radiology, Stanford University, Stanford, CA 94305.

Digital Object Identifier 10.1109/TUFFC.2008.715

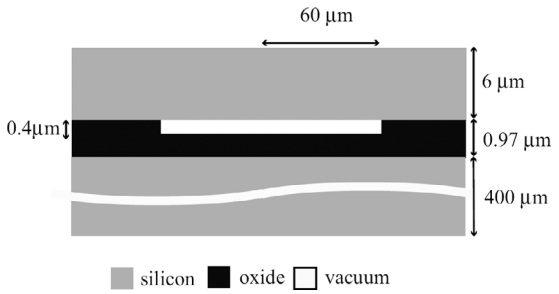

Fig. 1. Cross section of one cell of the CMUT transducer designed for HIFU operation at 2.5 MHz. Individual cells were fabricated in a close-packed structure to form a 2.51 mm by 2.32 mm transducer.

est and the constraints of the particular application. One example application we have discussed in previous conference publications is an 8-element, annular array for HIFU ablation of upper abdominal cancers [38], [39]. Other applications include intravascular ablations, such as cardiac ablation of arrhythmias [40].

While a focused transducer is our ultimate goal, in this first study, we used an unfocused test transducer to demonstrate that a CMUT could heat tissue-like material and that this heating could be monitored by MRI. Using an unfocused transducer is more challenging than using a focused transducer for several reasons. First, without focusing, heating tissues to high temperatures in short amounts of time is more difficult since the power density is not as concentrated. Thus, an unfocused CMUT needs to be efficient to heat tissue. Second, imaging close to a transducer is difficult if the transducer materials introduce artifacts into the image. In this study, we show that CMUTs demonstrate a good efficiency necessary for heating and produce minimal artifacts, which enables MR-temperature monitoring very close to the transducer. This paper is a continuation our conference proceeding [41].

II. Methods

The CMUT used for this experiment was fabricated using a high-temperature, direct fusion-bonding process described in [42]. Cells formed from this process consisted of a silicon dioxide cavity and electrically conductive silicon membrane. Individual cells (Fig. 1) were patterned into a 2.51 mm by 2.32 mm transducer. Because the silicon is highly electrically conductive, metal is not used on the membrane surfaces, which reduces electromigration effects during high power operation. Only small aluminum pads are needed for wire bonding the CMUT to a printed circuit board (PCB). In addition, silicon is very thermally conductive, which reduces self-heating effects that degrade transducer performance.

CMUTs are also MR-compatible. Silicon ($\chi = -6.52 \times 10^{-6}$) and silicon dioxide ($\chi = -16.3 \times 10^{-6}$) are level II compatible and produce no artifact; they have a susceptibility similar to that of tissue ($\chi = -7 \times 10^{-6}$ to -11×10^{-6}) and water ($\chi = -9.05 \times 10^{-6}$) [43]. Aluminum ($\chi = 20.7 \times 10^{-6}$) is not level II compatible [43];

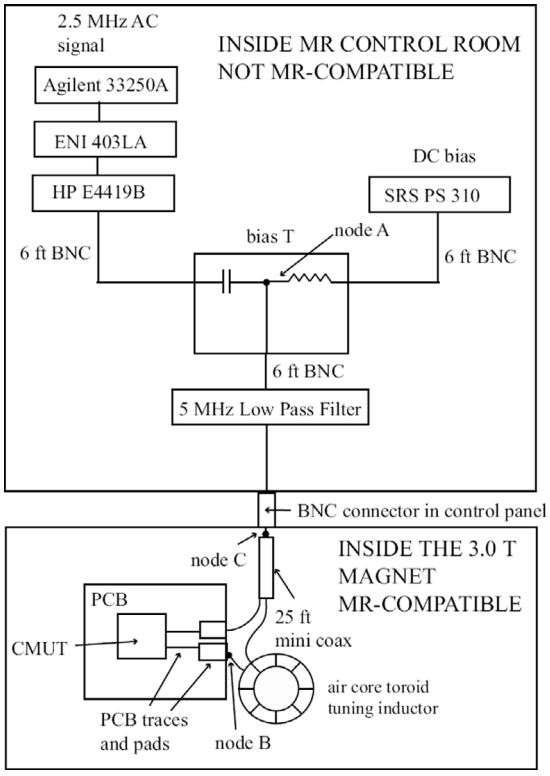

Fig. 2. Electrical setup in the magnet room and control room of the MR suite. The test equipment is not MR-compatible, so must be left inside the MR control room. Only an MR-compatible cable, an air core inductor, and the CMUT can be safely used inside the magnet.

because the CMUT is fabricated with conductive silicon membranes, no aluminum is used on the surface of the cells. The total volume of aluminum used in the bonding pads (150×150 μm and a thickness of 0.3 μm) is 2.0×10^{-14} m^2 or 5.6×10^{-9} kg, a negligible amount.

Because the test equipment was not MR-compatible, long lengths of cable were required to drive the CMUT in the 3.0 T magnet. The equipment was located on a cart in the MR control room. An arbitrary waveform generator (Agilent 33250A; Agilent Technologies, Inc., Palo Alto, CA), provided a CW, 2.5-MHz sinusoidal signal, which was then amplified by a 3-W amplifier (ENI 403LA; Electronic Navigation Industries, Richardson, TX). A power meter (HP E4419B; Hewlett Packard, Palo Alto, CA) was used to monitor the electrical power output from the amplifier. The AC signal was superimposed on the DC voltage at the bias T, which consisted of a DC blocking capacitor at the AC input port and a resistor, used for short circuit protection, at the DC voltage port. A bias voltage of 172 V was provided by a high voltage DC supply (SRS PS310; Stanford Research Systems, Stanford, CA). The combined signal was filtered using a custom-designed, 5-MHz low pass filter and connected through the panel in the control room; this grounded the drive system to the screen room. This low pass filter suppressed the high frequency noise components of the ENI amplifier, which creates noise at the nuclear resonance frequency and reduces the signal-to-noise ratio (SNR) of the MR image (Fig. 2).

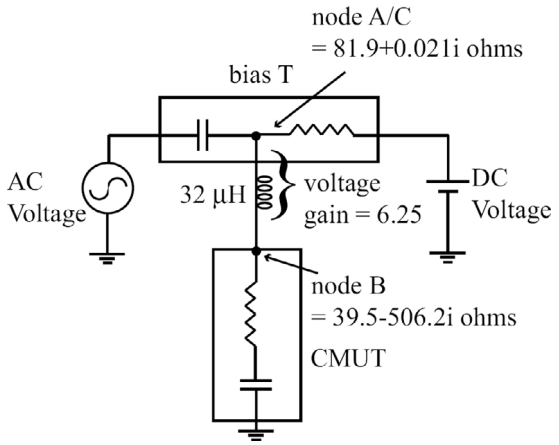

Fig. 3. Simplified electrical circuit used for driving the HIFU CMUT. The bias T superimposed the 172 V DC bias and the 2.5 MHz CW sinusoidal signal used to drive the CMUT. The inductor was used to tune the CMUT so that the reactive component of the impedance is zero at 2.5 MHz. The inductor also provides a voltage gain of 6.25.

All of the materials inside the magnet room and the 3.0 T magnet (126 MHz proton resonance frequency) needed to be MR-compatible and non-ferrous. A MR-compatible mini-coax (Belden Cable, St. Louis, MO) was used to connect the CMUT to the control panel inside the magnet room. We used an air-core toroid of approximately 32 μH to cancel the reactive component of the CMUT and to match the circuit as closely to 50 ohms as possible (Fig. 2). This makes it more efficient for the amplifier to drive the load.

Before the experiment, we characterized the CMUT and circuit outside the magnet room because our equipment was not MR-compatible. All of these measurements allowed us to calculate the power gain of the device during the experiment in the 3.0 T magnet. First, we measured the impedance at nodes C and B (Fig. 3) to use in power calculations. At 2.5 MHz, the low pass filter impedance was negligible, so nodes A and C have roughly the same impedance. We also characterized the voltage gain of the circuit from nodes A to B to be 6.25. This allowed us to monitor the CMUT during operation by observing the voltage at node A.

To avoid charging and breaking the actual device, we measured the output pressure of an identical device under the desired DC and AC driving voltage conditions using an calibrated piezoelectric hydrophone with 400-μm aperture (PZT_Z44_0400 hydrophone; Onda Corporation, Sunnyvale, CA). The device was first submerged in soybean oil (speed of sound of 1430 m/s and density of 930 kg/m^3) for electrical isolation. The hydrophone was placed 2 cm from the surface of the transducer and positioned laterally to find the largest pressure. Care was taken to make sure the hydrophone was properly aligned with the transducer face to minimize the errors. We accounted for the frequency response of the hydrophone [44], attenuation of the soybean oil (0.43 dB/cm at 2.5 MHz [45]), and diffraction [46] to calculate the pressure at the surface of the transducer. We did not account for nonlinear propagation and harmonics, which give a conservative estimate of the output pressure and thus the power of the transducer. The measured output pressure and the impedance of the soybean oil (Z = 1.45 MRayl) were used to calculate the average power density at the face of the transducer. Multiplying by the area of the device (5.8 mm^2) gave us the total acoustic output power.

We studied only one drive level for the CMUT in this experiment, corresponding to 172 V DC voltage (60% of collapse) and 250 Vpp AC voltage. In previous work, we found that a DC voltage of 60%, while applying as large an AC voltage as possible, produced the optimum output pressure [47]. The acoustic power is not linear with respect to the applied voltage because the electrostatic force exerted on the membrane is dependent on the square of the distance between the ground and top electrodes. The maximum output pressure is related to the balance between the DC operating point and the AC voltage applied. At higher DC voltages, the force and pressure per volt increases nonlinearly as the collapse voltage is reached. However, as the DC voltage approaches the collapse voltage, the amount of AC voltage that can be applied before the membrane collapses is smaller [47].

For MR imaging, the CMUT was placed in the 3.0 T GE scanner (Lucas Center, Stanford, CA) and 10 drops of soybean oil were dribbled on the surface for electrical insulation. A polyethylene bag isolated the oil layer and CMUT from the coupling gel (MediChoice, Mechanicsville, VA), which coupled the ultrasound energy into the 4-inch diameter, tissue-mimicking, HIFU phantom (ATS Laboratories, Inc., Bridgeport, CT). The opaque phantom has an acoustic attenuation of 0.503 dB/m/K, a speed of sound of 1538 m/s, a heat capacity of 3500 J/kg/K, and a thermal conductivity of 0.5 W/m/k. Since the phantom is water-based, the proton resonance frequency properties will resemble that of soft tissue. The coupling gel was applied directly from the bottle and not degassed; however, when placing the HIFU phantom on top of the oil and coupling gel, we exerted force to minimize the amount of coupling fluids between the phantom and the transducer and also to minimize the air pockets. Two imaging planes, coronal and sagittal, were measured in two different experiments using a 5 inch GE surface coil placed around the HIFU phantom (Fig. 4).

Before the heating experiment, we measured the susceptibility artifact of the CMUT to verify that it did not interfere with measurements of the heated region. To do this, we added a second phantom underneath the CMUT to identify the bottom surface of the printed circuit board on the image. We imaged the CMUT, with no applied voltage, in the sagittal plane using a fast gradient echo sequence with a transmit repetition time/transmit echo time (TR/TE) of 28.7/19.1 ms, the same sequence used for the thermal imaging.

During the heating, we used a fast gradient echo sequence with a TR/TE of 17.4/13.5 ms for the coronal plane and 28.7/19.1 ms for the sagittal plane. The magni-

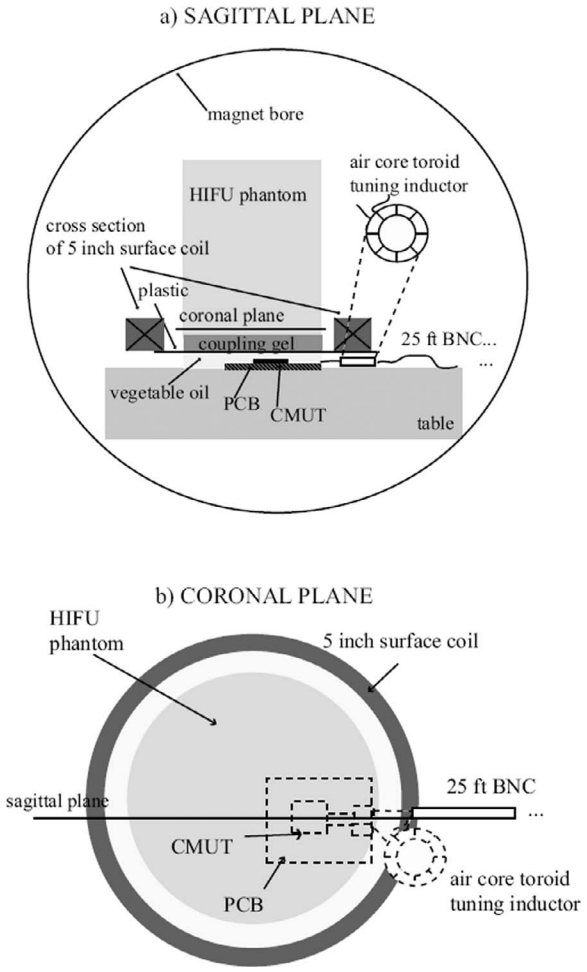

Fig. 4. Sagittal (a) and coronal (b) views of the setup used for MR-temperature mapping of the HIFU CMUT.

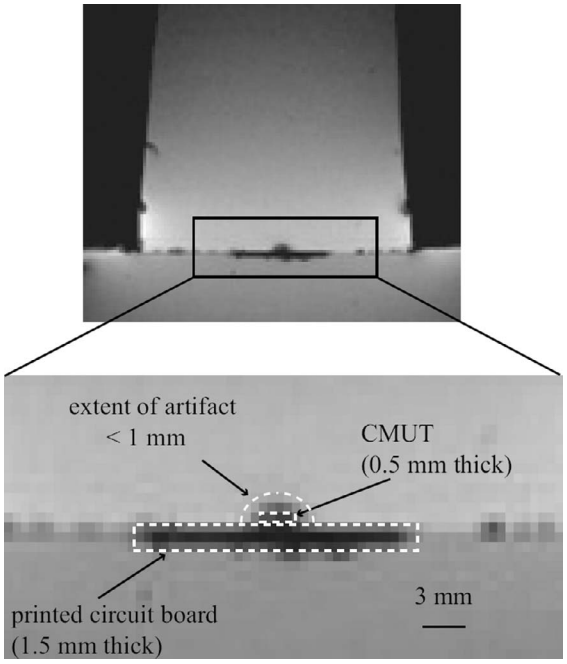

Fig. 5. Measurement in the sagittal plane o of the artifact caused by the CMUT.

tude, phase, real, and imaginary results were saved from the scan. One hundred images per series were captured for 7.5 and 12.5 minutes for the coronal and sagittal planes, respectively. During this imaging time, we applied 2.5 min and 5 min of therapy at 2.5 MHz for the coronal and sagittal planes, respectively. Each image was 256 by 256 pixels, with a spatial resolution of 0.7 mm in the coronal images and 0.9 mm in the sagittal images.

The proton resonance frequency shift due to temperature was observed as a change in phase, $\triangle\phi$, that we calculated by subtracting successive images from the first image. The change in temperature, $\triangle T$, was then calculated using the following equation [48]:

$$\triangle T = \frac{\triangle\phi}{\alpha 2\pi\bar{\gamma} B_0 TE}, \tag{1}$$

where the proton resonance shift α is 0.01 ppm/°C, the proton resonance frequency γ is 26734 rad/sec/G, the magnetic field strength B_0 is 3.0 T, and the transmit echo time (TE) is given by the scan parameters mentioned previously. The temperature coefficient α is stable for temperatures under focused ultrasound application [49]. To account for baseline drift of the MR image over time, we averaged the phase difference in a 1.5 cm by 1.5 cm region of the phantom far from the heated region; this phase difference was then subtracted from $\triangle\phi$ before the temperature was calculated. The temperature error was determined by calculating the standard deviation of the temperature map before heating. This standard deviation was calculated in a 1.5 cm by 1.5 cm area that encompassed the region of interest where heating would occur.

The cumulative equivalent minutes at 43°C (CEM_{43}) was then calculated assuming a temperature rise from 37°C. The CEM_{43} is given by the following equation [50]:

$$\mathrm{CEM}_{43} = \sum_t R^{(43-T(t))} \triangle t, \tag{2}$$

where $R = 0.25$ if $T(t) < 43$ and $R = 0.5$ if $T(t) > 43$.

This assumes that heating of a room-temperature, tissue-mimicking phantom requires roughly the same amount of power as heating a 37°C phantom. Heating tissue is reliant on the attenuation and speed of sound of the tissue; between 20°C and 37°C, the speed of sound and the attenuation show a change of less than 10% [51], [52]. The attenuation increases rapidly at temperatures greater than 50°C because of protein denaturation. This increase in attenuation will cause an even greater degree of heating. This means that by starting at a lower temperature, we are effectively underestimating our heating and necrosis threshold.

III. Results and Discussion

We first measured the susceptibility artifact of the device with no applied power. We found that the artifact extended at most 1 mm from the surface of the CMUT

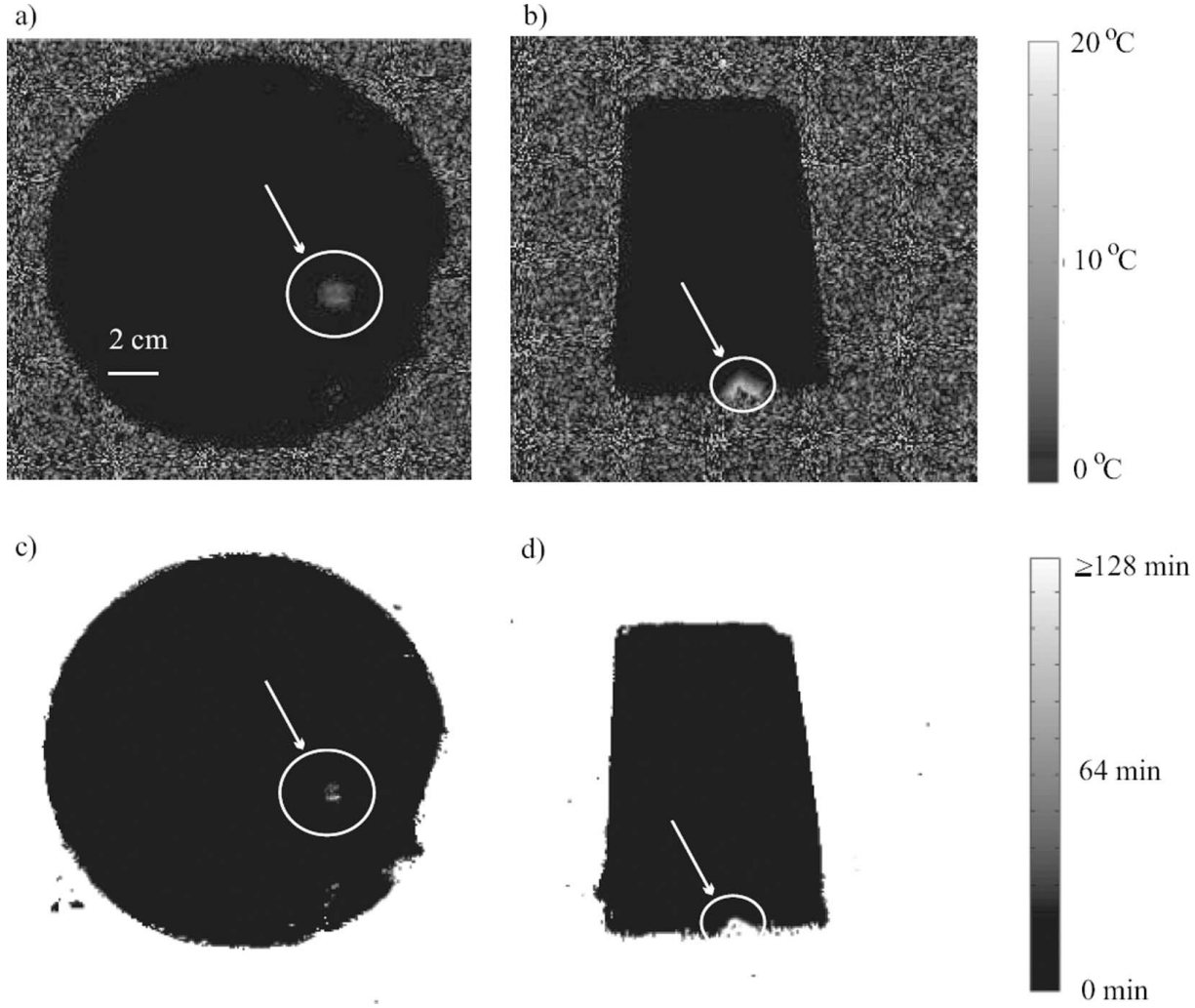

Fig. 6. Coronal (a) and sagittal (b) temperature maps at the end of the heating time period, at 2.5 and 5 min, respectively. Calculated CEM_{43} for the corononal (c) and sagittal (d) images, which shows that some areas reach 128 equivalent minutes at the end of the heat. This is enough to necrose heat tissue.

(Fig. 5). Given that we measured the coronal slice 3–6 mm away from the device surface and that the heating areas in both slices extend far past 1 mm, our temperature maps in those locations are not impacted by susceptibility artifacts.

Next, we evaluated the performance of the CMUT by calculating efficiencies and also observing the temperature rise of the phantom under MR temperature guidance. To evaluate the effectiveness of the tuning circuit, we calculated the electrical efficiency, defined as the electrical power delivered to the CMUT compared to the electrical power supplied by the amplifier. We found the electrical efficiency by measuring the applied voltage at node A (Fig. 2) and calculating the delivered power to the CMUT using the impedance measured at nodes A and B. With normal care in calibration, it is possible to measure impedance with errors of less than 1%. Though 2.5 W was measured from the output of the amplifier, only 1.19 W of electrical power was delivered to the CMUT, which is an electrical efficiency of 48%. The cable, connections, and inductor have parasitics, which cause this loss.

From the hydrophone measurement, under 172 Vbias and 250 Vpp AC voltage, the CMUT showed a surface output pressure of 1.3 MPa peak to peak and an acoustic output power of 0.8 W in immersion. Since 1.19 W of electrical power was supplied to the CMUT, the electrical-to-acoustical efficiency of the CMUT is thus 68%. Though the hydrophone is calibrated by the manufacturer (Onda Corporation, Sunnyvale, CA), there are still errors associated with the accuracy of the acoustic pressure measurement, and thus the accuracy of the calculated acoustic output power. Though we took care to align the hydrophone with the transducer, tilt and positioning errors will cause the measured output pressure to be less than the maximum. This will cause us to underestimate our efficiency. However, because the transducer is unfocused, its beamwidth is large at 2 cm, compared to the size of the hydrophone, so the error will be minimal.

Already, this unfocused CMUT transducer was efficient enough to produce a maximum temperature rise in the HIFU phantom of 14.6°C in the coronal plane after 2.5 min of heating [Fig. 6(a)]. In measurements of the sagittal

plane, 18.6°C temperature rise was achieved after 5 min of heating [Fig. 6(b)]. Approximately 200 voxels were in the heated area of each image. The standard deviation of the temperature maps, which indicates the uncertainty and error in the temperature measurement, was 0.7°C and 0.8°C in the coronal and sagittal planes, respectively. This error is only 5%, compared to the maximum temperature rise.

These temperature rises are reasonable for unfocused ultrasound; a change in temperature of over 13°C would raise the body temperature above 50°C, which causes coagulative necrosis [53], [54]. Using the CEM_{43}, we quantified the degree of necrosis as a function of temperature and time. The maximum CEM_{43} reached by any pixel in the treatment region was 252 and 6230 equivalent minutes in the coronal and sagittal planes, respectively. Looking only at the pixels that reached the 128 equivalent minute [55] threshold for myocardial necrosis [Fig. 6(c), (d)], we found that this device could potentially necrose cardiac tissue to a depth of approximately 1 cm, discounting the effects of perfusion. Because the HIFU phantom does not simulate perfusion, the heating and temperature rise *in vivo* will be less than what we measured in the phantom. To deliver more power and overcome perfusion to necrose tissue in shorter amounts of time, we will develop a focused transducer design.

IV. Conclusion

We have demonstrated that CMUTs can be used to heat an HIFU phantom with unfocused ultrasound by 14–18°C over a 2.5–5 min time period. This CMUT demonstrated an MR artifact of less than 1 mm radially from its surface and was successfully monitored using MR-temperature maps. Though the temperature rise in an unperfused, HIFU phantom from this unfocused transducer is relatively small, the heating produced a CEM_{43} of over 128 min near the transducer. This is the threshold necrosis value for cardiac tissue. These first experimental results and MR-temperature maps are promising for the further development of CMUTs in ultrasonic therapeutics.

In the future, we aim to build a ring annular focused transducer for cancer ablation, which will enable greater heating in shorter periods of time, even with perfused tissue. We also plan to improve our electrical boards and connections to reduce radio frequency noise and induction of eddy currents. We can do this by reducing the electrical loops in our circuit and designing a new tuning circuit that does not require such a large inductor.

References

[1] G. ter Haar, "Ultrasound focal beam surgery," *Ultrasound Med. Biol.*, vol. 21, no. 5, pp. 1089–1100, 1995.

[2] W. J. Fry, W. H. Mosberg, J. W. Barnard, and F. J. Fry, "Production of focal destructive lesions in the central nervous system with ultrasound," *J. Neurosurg.*, vol. 11, pp. 471–478, 1954.

[3] W. J. Fry, W. H. Mosberg, J. W. Barnard, and F. J. Fry, "Ultrasonic lesions in the central nervous system with ultrasound," *Science*, vol. 122, pp. 517–518, 1955.

[4] J. E. Zimmer, K. Hynynen, F. Marcus, and D. S. He, "The feasibility of using ultrasound for cardiac ablation," in *Proc. IEEE Ultrason. Symp.*, 1993, pp. 1203–1206.

[5] K. L. Gentry and S. W. Smith, "Integrated catheter for 3-D intracardiac echocardiography and ultrasound ablation," *IEEE Trans. Ultrason., Ferroelect., Freq. Contr.*, vol. 51, no. 7, pp. 800–808, 2004.

[6] M. D. Lesh, J. M. Kalman, and M. R. Karch, "Use of intracardiac echocardiography during electrophysiologic evaluation and therapy of atrial arrhythmias," *J. Cardiovasc. Electrophysiol.*, vol. 9, (suppl. 8), pp. S40–S47, 1998.

[7] J.-U. Kluiwstra, Y. Zhang, P. VanBaren, S. A. Strickberg, E. S. Ebbini, and C. A. Cain, "Ultrasound phased arrays for noninvasive myocardial ablation: Initial studies," in *Proc. IEEE Ultrason. Symp.*, vol. 2, 1995, pp. 1605–1608.

[8] F. P. Curra and L. A. Crum, "Therapeutic ultrasound: Surgery and drug delivery," *Acoust. Sci. Technol.*, vol. 24, no. 6, pp. 343–348, 2003.

[9] S. Vaezy, R. Martin, H. Yaziji, P. Kaczkowski, G. Keilman, S. Carter, M. Caps, E. Y. Chi, M. Bailey, and L. Crum, "Hemostasis of punctured blood vessels using high-intensity focused ultrasound," *Ultrasound Med. Biol.*, vol. 24, pp. 903–910, 1998.

[10] V. Zderic, A. Keshavarzi, M. L. Noble, M. Paun, S. R. Sharar, L. A. Crum, R. W. Martin, and S. Vaezy, "Hemorrhage control in arteries using high-intensity focused ultrasound: A survival study," *Ultrasonics*, vol. 44, pp. 46–53, 2006.

[11] J. E. Kennedy, G. Ter Haar, and D. Cranston, "High intensity focused ultrasound: Surgery of the future?," *Br. J. Radiol.*, vol. 76, pp. 590–599, 2003.

[12] F. A. Jolesz and K. Hynynen, "Magnetic resonance image-guided focused ultrasound surgery," *Cancer J.*, vol. 8, (suppl. 1), pp. S100–S112, 2002.

[13] F. A. Jolesz, K. Hynynen, N. McDannold, D. Freundlich, and D. Kopelman, "Noninvasive thermal ablation of hepatocellular carcinoma by using magnetic resonance imaging-guided focused ultrasound," *Gastroenterology*, vol. 127, (suppl. 1), pp. S242–S247, 2004.

[14] C. M. Tempany, E. A. Stewart, N. McDannold, B. J. Quade, F. A. Jolesz, and K. Hynynen, "MR imaging-guided focused ultrasound surgery of uterine leiomyomas: A feasibility study," *Radiology*, vol. 226, no. 3, pp. 897–905, 2003.

[15] K. Hynynen, O. Pomeroy, D. N. Smith, P. E. Huber, N. J. McDannold, J. Kettenbach, J. Baum, S. Singer, and F. A. Jolesz, "MR imaging-guided focused ultrasound surgery of fibroadenomas in the breast: A feasibility study," *Radiology*, vol. 219, no. 1, pp. 176–185, 2001.

[16] K. Hynynen, V. Colucci, A. Chung, and F. Jolesz, "Noninvasive arterial occlusion using MRI-guided focused ultrasound," *Ultrasound Med. Biol.*, vol. 22, no. 8, pp. 1071–1077, 1996.

[17] D. R. Daum, N. B. Smith, R. King, and K. Hynynen, "In vivo demonstration of noninvasive thermal surgery of the liver and kidney using an ultrasound phased array," *Ultrasound Med. Biol.*, vol. 25, no. 7, pp. 1087–1098, 1999.

[18] H. E. Cline, K. Hynynen, C. J. Hardy, R. D. Watkins, J. F. Schenck, and F. A. Jolesz, "MR temperature mapping of focused ultrasound surgery," *Magn. Reson. Med.*, vol. 31, no. 6, pp. 628–636, 1994.

[19] V. Rieke, K. K. Vigen, G. Sommer, B. L. Daniel, J. M. Pauly, and K. Butts, "Referenceless PRF shift thermometry," *Magn. Reson. Med.*, vol. 51, no. 6, pp. 1223–1231, 2004.

[20] K. Butts, S. J. Riederer, R. L. Ehman, R. M. Thompson, and C. R. Jack, "Interleaved echo planar imaging on a standard MRI system," *Magn. Reson. Med.*, vol. 31, no. 1, pp. 67–72, 1994.

[21] H. E. Cline, J. F. Schenck, K. Hynynen, R. D. Watkins, S. P. Souza, and F. A. Jolesz, "MR-guided focused ultrasound surgery," *J. Comput. Assist. Tomogr.*, vol. 16, pp. 956–965, 1992.

[22] J. S. Lewin, C. A. Petersilge, S. F. Hatem, J. L. Duerk, G. Lenz, M. E. Clampitt, M. L. Williams, K. R. Kaczynski, C. F. Lanzieri, A. L. Wise, and J. R. Haaga, "Interactive MR imaging-guided biopsy and aspiration with a modified clinical C-arm system," *Am. J. Roentgenol.*, vol. 170, no. 6, pp. 1593–1601, 1998.

[23] T. J. Vogl, "Laser-induced thermotherapy: Do we really need MR thermometry?," *Eur. Radiol.*, vol. 12, no. 1, pp. 5–6, 2002.

[24] S. Rossi, M. Di Stasi, E. Buscarini, P. Quaretti, F. Garbagnati, L. Squassante, C. T. Paties, D. E. Silverman, and L. Buscarini, "Percutaneous RF interstitial thermal ablation in the treatment of hepatic cancer," *Am. J. Roentgenol.*, vol. 167, no. 3, pp. 759–768, 1996.

[25] W. J. Fry, "Precision high intensity focusing ultrasonic machines for surgery," *Am. J. Phys. Med.*, vol. 37, pp. 152–156, 1958.

[26] I. H. Rivens, R. L. Clark, and G. R. ter Haar, "Design of focused ultrasound surgery transducers," *IEEE Trans. Ultrason., Ferroelect., Freq. Contr.*, vol. 43, no. 6, pp. 1023–1031, 1966.

[27] S. Zhang, R. Xia, L. Lebrun, D. Anderson, and T. R. Shrout, "Piezoelectric materials for high power, high temperature applications," *Mater. Lett.*, vol. 59, no. 27, pp. 3471–3475, 2005.

[28] J. Y. Chapelon, D. Cathignol, C. Cain, E. Ebbini, J. U. Kluiwstra, O. A. Sapozhnikov, G. Fleury, R. Berriet, L. Chupin, and J. L. Guey, "New piezoelectric transducers for therapeutic ultrasound," *Ultrasound Med. Biol.*, vol. 26, no. 1, pp. 153–159, 2000.

[29] J. E. Zimmer, K. Hynynen, D. S. He, and F. Marcus, "The feasibility of using ultrasound for cardiac ablation," *IEEE Trans. Biomed. Eng.*, vol. 42, no. 9, pp. 891–897, 1995.

[30] D. L. Deardorff and C. J. Diederich, "Ultrasound applicators with internal water-cooling for high-powered interstitial thermal therapy," *IEEE Trans. Biomed. Eng.*, vol. 47, no. 10, pp. 1356–1365, 2000.

[31] M. D. Brentnall, R. W. Martin, S. Vaezy, P. Kaczkowski, F. Forster, and L. Crum, "A new high intensity focused ultrasound applicator for surgical applications," *IEEE Trans. Ultrason., Ferroelect., Freq. Contr.*, vol. 48, no. 1, pp. 53–63, 2001.

[32] E. Ebbini, J. C. Bischof, and J. E. Coad, "Lesion formation and visualization using dual-mode ultrasound phased arrays," in *Proc. IEEE Ultrason. Symp.*, vol. 2, 2001, pp. 1351–1354.

[33] H. Wan, P. VanBaren, E. S. Ebbini, and C. A. Cain, "Ultrasound surgery: Comparison of strategies using phased array systems," *IEEE Trans. Ultrason., Ferroelect., Freq. Contr.*, vol. 43, no. 6, pp. 1085–1098, 1996.

[34] J. S. Tan, L. A. Frizzell, N. Sanghvi, S.-J. Wu, R. Seip, and J. T. Kouzmanoff, "Ultrasound phased arrays for prostate treatment," *J. Acoust. Soc. Amer.*, vol. 109, no. 6, pp. 3055–3064, 2001.

[35] A. S. Ergun, Y. Huang, X. Zhuang, O. Oralkan, G. G. Yaralioglu, and B. T. Khuri-Yakub, "Capacitive micromachined ultrasonic transducers: Fabrication technology," *IEEE Trans. Ultrason., Ferroelect., Freq. Contr.*, vol. 52, no. 12, pp. 2242–2258, 2005.

[36] I. Ladabaum, X. C. Jin, H. T. Soh, A. Atalar, and B. T. Khuri-Yakub, "Surface micromachined capacitive ultrasonic transducers," *IEEE Trans. Ultrason., Ferroelect., Freq. Contr.*, vol. 45, no. 3, pp. 678–690, 1998.

[37] G. G. Yaralioglu, A. S. Ergun, B. Bayram, E. Haeggstrom, and B. T. Khuri-Yakub, "Calculation and measurement of electromechanical coupling coefficient of capacitive micromachined ultrasonic transducers," *IEEE Trans. Ultrason., Ferroelect., Freq. Contr.*, vol. 50, no. 4, pp. 449–456, 2003.

[38] S. H. Wong, A. S. Ergun, G. G. Yaralioglu, O. Oralkan, E. Liu, M. Kupnik, R. K. Butts, and B. T. Khuri-Yakub, "Capacitive micromachined ultrasonic transducers for high intensity focused ablation of upper abdominal tumors," in *Proc. IEEE Ultrason. Symp.*, 2006, pp. 841–844.

[39] S. H. Wong, A. S. Ergun, G. G. Yaralioglu, O. Oralkan, M. Kupnik, R. K. Butts, and B. T. Khuri-Yakub, "Design of HIFU CMUT arrays for treatment of liver and renal cancer," in *Proc. 6th AIP Int. Therapeut. Ultrasound Symp.*, vol. 911, 2007, pp. 54–60.

[40] S. H. Wong, I. O. Wygant, D. T. Yeh, X. Zhuang, B. Bayram, M. Kupnik, O. Oralkan, A. S. Ergun, G. G. Yaralioglu, and B. T. Khuri-Yakub, "Capacitive micromachined ultrasonic transducer arrays for integrated diagnostic/therapeutic catheters," in *Proc. 5th AIP Int. Therapeut. Ultrasound Symp.*, vol. 829, 2006, pp. 395–399.

[41] S. H. Wong, M. Kupnik, K. Butts Pauly, and B. T. Khuri-Yakub, "Advantages of capacitive micromachined ultrasonics transducers (CMUTs) for high intensity focused ultrasound (HIFU)," in *Proc. IEEE Ultrason. Symp.*, 2007, pp. 1313–1316.

[42] Y. Huang, A. S. Ergun, E. Haeggstrom, M. H. Badi, and B. T. Khuri-Yakub, "Fabricating capacitive micromachined ultrasonic transducers with wafer-bonding technology," *Microelectromech. Syst.*, vol. 12, no. 2, pp. 128–137, 2003.

[43] J. F. Schenck, "The role of magnetic susceptibility in magnetic resonance imaging: MRI magnetic compatibility of the first and second kinds," *Med. Phys.*, vol. 23, no. 6, pp. 815–850, 1996.

[44] http://www.ondacorp.com/.

[45] O. Oralkan, A. S. Ergun, J. A. Johnson, M. Karaman, U. Demirci, K. Kaviani, T. H. Lee, and B. T. Khuri-Yakub, "Capacitive micromachined ultrasonic transducers: Next-generation arrays for acoustic imaging," *IEEE Trans. Ultrason., Ferroelect., Freq. Contr.*, vol. 49, no. 11, pp. 1596–1610, 2002.

[46] G. S. Kino, *Acoustic Waves: Devices, Imaging, and Analog Signal Processing.* Englewood Cliffs, NJ: Prentice-Hall, 1987.

[47] G. G. Yaralioglu, B. Bayram, and B. T. Khuri-Yakub, "Finite element analysis of CMUTs: Conventional vs. collapse operation modes," in *Proc. IEEE Ultrason. Symp.*, 2006, pp. 586–589.

[48] Y. Ishihara, A. Calderon, H. Watanabe, K. Okamoto, Y. Suzuki, K. Kuroda, and Y. Suzuki, "A precise and fast temperature mapping using water proton chemical shift," *Magn. Reson. Med.*, vol. 34, pp. 814–823, 1995.

[49] T. Wu, K. R. Kendell, J. P. Felmlee, B. D. Lewis, and R. L. Ehman, "Reliability of water proton chemical shift temperature calibration for focused ultrasound ablation therapy," *Med. Phys.*, vol. 27, no. 1, pp. 221–224, 2000.

[50] S. A. Sapareto and W. C. Dewey, "Thermal dose determination in cancer therapy," *Int. J. Radiat. Oncol. Biol. Phys.*, vol. 10, pp. 787–800, 1984.

[51] J. C. Bamber and C. R. Hill, "Ultrasonic attenuation and propagation speed in mammalian tissues as a function of temperature," *Ultrasound Med. Biol.*, vol. 5, pp. 149–157, 1979.

[52] U. Techavipoo, T. Varghese, Q. Chen, T. A. Stiles, J. A. Zagzebski, and G. R. Frank, "Temperature dependence of ultrasonic propagation speed and attenuation in excised canine liver tissue measured using transmitted and reflected pulses," *J. Acoust. Soc. Amer.*, vol. 115, no. 6, pp. 2859–2865, 2004.

[53] M. H. Seegenschmiedt, P. Fessenden, and C. Vernon, *Principles and Practices of Thermoradiotherapy and Thermochemotherapy.* Berlin: Springer-Verlag, 1995.

[54] F. S. Foster, R. M. Henkelman, and D. B. Plewes, "Quantifying tissue damage due to focused ultrasound heating observed by MRI," *Magn. Reson. Med.*, vol. 41, pp. 321–328, 1999.

[55] D. Haemmerich, J. G. Webster, and D. M. Mahvi, "Thermal dose versus isotherm as lesion boundary estimator for cardiac and hepatic radio-frequency ablation," in *Proc. 25th Int. Conf. IEEE Eng. Med. Biol. Soc.*, 2003, pp. 134–136.

Serena Wong was born in Stanford, CA. She received her B.S. and M.S. degrees in electrical engineering from Stanford University, Stanford, CA, in 2002 and 2003, respectively. She is currently a Ph.D. candidate in electrical engineering at the Edward L. Ginzton Laboratory of Stanford University. She is a 2002 National Science Foundation Fellow, 2002 Stanford Graduate Fellow, and a member of Tau Beta Pi.

From 1998 through 2001, she worked as a research assistant in the Pre-polarized Magnetic Resonance Imaging (pMRI) laboratory at Stanford University in an effort to develop a cost-effective MRI system. This system would greatly reduce costs of imaging technology and improve accessibility for patients. Recently, she has been interested in high intensity focused ultrasound (HIFU) as a minimally-invasive therapeutic tool for treatment of cancer. She is presently working with capacitive micromachined ultrasonic transducers (CMUTs) for HIFU applications such as the treatment of lower abdominal cancers.

Ronald D. Watkins is a Senior Scientific Research Associate in the Stanford School of Medicine and works in the Richard M. Lucas Center for Radiological Sciences and the Edward L. Ginzton Lab of Applied Physics. Before joining Stanford, he worked at General Electric Medical Systems in Rancho Cordova, CA, and GE Corporate Research in Niskayuna, NY. Early in his career he focused on digital X-Ray image processing, CT Data Acquisition, and MRI subsystems. He then moved to Ultrasound imaging systems and developed systems for MR Guided Focused Ultrasound Surgery and Very High Field MR Imaging Systems. He has 37 issued US Patents and 46 external publications and conference proceedings. He is a member of the IEEE and the ISMRM.

Mario Kupnik is currently a research associate in electrical engineering at Edward L. Ginzton Laboratory at Stanford University. He received his Ph.D. degree from the University of Leoben, Austria, in 2004, and the Diplom Ingenieur degree from Graz University of Technology, in 2000. From summer 1999 to October 2000, he worked as an Analog Design Engineer for Infineon Technologies AG, Graz, on the design of ferroelectric memories and contactless smart card (RFID) systems. His present research interests include the design, modeling, fabrication, and application of micromachined sensors and actuators, with a main focus on capacitive micromachined ultrasonic transducers mainly for air-coupled applications, including high gas temperatures. Examples are transit-time gas flowmeters for hot and pulsating gases, ultrasonic nondestructive evaluation using non-contact ultrasound, nonlinear acoustics, and bio/chemical gas sensing applications (electronic nose). Dr. Kupnik has more than 5 years teaching experience in the field of electrical engineering and he is a member of the IEEE.

Kim Butts Pauly received a B.S. degree in physics from Duke University, Durham, NC. She received her Ph.D. in biophysical sciences from the Mayo Graduate School in Rochester, MN. In 1996, she joined the faculty at Stanford University's Department of Radiology, where she has been working on MR-guided high intensity focused ultrasound, cryoablation, RF ablation, and biopsy. She has also been involved with the development of a truly integrated X-Ray and MRI system.

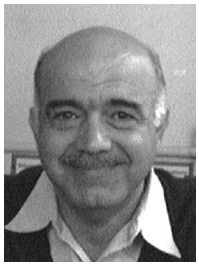

Butrus T. (Pierre) Khuri-Yakub (S'70–S'73–M'76–SM'87–F'95) is a Professor of Electrical Engineering at Stanford University. He received the B.S. degree in 1970 from the American University of Beirut, the M.S. degree in 1972 from Dartmouth College, and the Ph.D. degree in 1975 from Stanford University, all in electrical engineering. He was a Research Associate (1965–1978) then Senior Research Associate (1978–1982) at the E. L. Ginzton Laboratory of Stanford University and was promoted to the rank of Professor of Electrical Engineering in 1982. His current research interests include medical ultrasound imaging and therapy, micromachined ultrasonic transducers, smart bio-fluidic channels, microphones, ultrasonic fluid ejectors, and ultrasonic nondestructive evaluation, imaging and microscopy. He has authored over 400 publications and has been principal inventor or co-inventor of 76 US and International issued patents. He was awarded the Medal of the City of Bordeaux in 1983 for his contributions to Nondestructive Evaluation, the Distinguished Advisor Award of the School of Engineering at Stanford University in 1987, the Distinguished Lecturer Award of the IEEE UFFC society in 1999, a Stanford University Outstanding Inventor Award in 2004, and a Distinguished Alumnus Award of the School of Engineering of the American University of Beirut in 2005.